# Characterization of topoisomerase II–DNA interaction and identification of a DNA-binding domain by ultraviolet laser crosslinking

Franki Hung[a,**], Dan Luo[b,*], Debra M. Sauvé[a], Mark T. Muller[b], Michel Roberge[a,*]

[a]*Department of Biochemistry and Molecular Biology, University of British Columbia, Vancouver, B.C. V6T 1Z3, Canada*
[b]*Department of Molecular Genetics, Ohio State University, Columbus, OH 43210, USA*

Received 7 November 1995; revised version received 4 January 1996

**Abstract We have used ultraviolet laser crosslinking to characterize the DNA-binding properties of highly purified yeast topoisomerase II in the absence of ATP. A single 5 ns, 20 mJ pulse of 266 nm light produced optimal crosslinking to a short DNA duplex, with an efficiency of 0.25%. An equilibrium binding constant ($K_{eq}$) of $1.2 \pm 0.5 \times 10^8$ $M^{-1}$ was determined from kinetic analysis. Topoisomerase II showed highest affinity for supercoiled DNA. Limited proteolysis of crosslinked topoisomerase II–DNA complexes showed a site of crosslinking to be within a 29-kDa fragment with Leu-681 at its amino-terminal end. This region contains the active Tyr-783 and is homologous to the amino-terminal region of the DNA-binding bacterial gyrase GyrA subunit, suggesting a conserved DNA-binding mechanism.**

*Key words:* Topoisomerase II; DNA-binding; Ultraviolet laser crosslinking; *Saccharomyces cerevisiae*

## 1. Introduction

DNA topoisomerase II (topo II) changes DNA topology by passing one DNA duplex through another [1]. Topo II plays an essential role in chromosome segregation [2–4], chromosome condensation [3], and the resolution of recombined chromosomes in meiosis [5] and has also been implicated in many other processes associated with DNA (reviewed in [6]).

The topo II catalytic reaction is complex and involves noncovalent binding of the enzyme to DNA, often at crossovers [7,8], followed by cleavage of the two DNA strands, which is accompanied by covalent attachment of the enzyme to DNA, religation of the DNA breaks, and return to the active enzyme conformation in a reaction that requires ATP hydrolysis (reviewed in [9]).

In eukaryotes, topo II is a dimer composed of two identical subunits about 1500 amino acids long and contains no obvious DNA-binding motifs. The N-terminal 76 amino acid residues and C-terminal 260 amino acid residues of fission yeast topo II appear to be dispensable for enzymatic activity in vitro, implying that DNA-binding domains do not lie in these regions [10]. Topo II is conserved among eukaryotes and also has significant sequence similarity to bacterial gyrase and phage T4 topo II subunits [10,11]. Structural and functional features of regions within topo II have been inferred from comparison of the predicted amino acid sequence of several eukaryotic topo II genes with that of prokaryotic topoisomerases and resolvases, whose properties have been studied in more detail. The N-terminal half of eukaryotic topo II has similarity to GyrB (Fig. 4) and phage gp39 and gp60, which are involved in ATP-binding [10]. On the basis of high conservation of certain amino acid stretches, Caron and Wang [12] have proposed that a region of topo II encompassing the C-terminal part of the GyrB-like domain may participate in binding to DNA. The central region of topo II has similarly been proposed to participate in binding DNA because of its similarity to the N-terminal domain of GyrA (Fig. 4) and phage gp52, which are involved in binding DNA and in the catalytic reaction [10]. The C-terminal 15% of topo II has short regions of similarity with histone H1 characterized by matching lysine-rich regions, suggesting that it may also interact with DNA [13]. However, this domain has no homology to prokaryotic topoisomerases.

Here, we report the use of single-pulse ultraviolet (UV) laser crosslinking to characterize the interaction of topo II with DNA and to identify a DNA-binding domain.

## 2. Materials and methods

### 2.1. Materials

Plasmid pRYG contains a 54-base pairs (bp) sequence of alternating purines and pyrimidines that constitutes a strong topo II cleavage site [14]. It was obtained in supercoiled or relaxed form from TopoGEN (Columbus, OH). Linear pRYG was obtained by digestion with *Hin*dIII followed by phenol extraction and ethanol purification. Two oligodeoxyribonucleotide duplexes were synthesized by the Nucleic Acids Protein Service, University of British Columbia by standard methods: 5′-CACACATACATATACATATATATGCATTCATT-3′ is termed 'RY oligo' and contains part of the alternating purine/pyrimidine sequence from pRYG, and 5′-TGGATTAAAACCTTCTGGTAAGAAAAGAAAAA-3′, is termed 'non-RY oligo' and corresponds to an adjacent region in pRYG that does not contain any topo II cleavage sites [14].

*S. cerevisiae* topo II was overexpressed in yeast from plasmid pYepyt2 and purified according to a modification of [15]. Briefly, yeast was grown in raffinose to saturation and 2% galactose was added for 4–6 h. The cells were harvested by centrifugation, washed with cold TGEP (0.1 M Tris-HCl, pH 7.6, 10% glycerol, 1 mM EDTA, 1 mM EGTA, 1 μM β-mercaptoethanol, 0.5 mM sodium bisulfite) and lysed with glass beads. After centrifugation at $800 \times g$ for 5 min, the supernatant was recovered and further centrifuged at $50{,}000 \times g$ for 15 min at 4°C. The pellet was suspended in TGEP containing 0.4 M NaCl and left on ice for 1 h. After centrifugation at $100{,}000 \times g$ for 60 min at 4°C, the supernatant was diluted with an equal volume of cold TGEP and loaded onto a 2.6 × 12 cm Biorex 70 column. The column was washed with 60 ml of TGEP containing 0.2 M NaCl and topo II was eluted with a linear gradient of 0.2 to 1.0 M NaCl in TGEP. Active fractions were pooled and diluted 4-fold with TGEP before loading onto a Mono-Q FPLC column. A linear gradient of 5 to 500 mM NaCl was applied and topo II eluted at about 300 mM NaCl. Purity was evaluated by sodium

*Corresponding author. Fax: (1) (604) 822-5227.

**These authors contributed equally.

*Abbreviations:* bp, base pair; oligo, oligodeoxyribonucleotide duplex; PAGE, polyacrylamide gel electrophoresis; SDS, sodium dodecyl sulfate; topo, DNA topoisomerase; UV, ultraviolet.


*SSDI* 0014-5793(96)00035-X

dodecyl sulfate (SDS) polyacrylamide gel electrophoresis (PAGE) (Fig. 1A). The purest fraction, labelled 'b' in Fig. 1A, contains a single homogenous band and was used for crosslinking experiments. V8 protease was purchased from Promega, [$\gamma$-$^{32}$P]ATP from NEN, and micrococcal nuclease and polynucleotide kinase from Pharmacia.

*2.2. Binding and UV irradiation*

Standard binding reactions were performed using 11 nM topo II and 25 nM RY oligo in 50 mM Tris-HCl (pH 8.0) and 0.5 mM EDTA in a total volume of 25 $\mu$l. After 3 min incubation at ambient temperature, the samples were irradiated with a single pulse of 266 nm light emitted from a Nd:YAG laser [16]. The pulse was 5–6 ns long, and its energy was 20 mJ. In most experiments, the RY oligo had been end-labelled using [$\gamma$-$^{32}$P]ATP and polynucleotide kinase, and purified by reversed-phase chromatography on Sep-Pak $C_{18}$ columns [17].

*2.3. V8 protease digestion of crosslinked complexes*

Scaled-up reactions contained 11 nM topo II and 25 nM RY oligo in 50 mM Tris-acetate (pH 7.5) and 0.5 mM EDTA in a volume of 400 $\mu$l. After 3 min incubation at ambient temperature, 50 $\mu$l aliquots were each irradiated with a single 50 mJ pulse. $CaCl_2$ was then added to a final concentration of 2 mM and the pooled samples were incubated with a large excess of micrococcal nuclease (6.25 U/ml, 19 U/mg) for 30 min at 37°C. The samples were then adjusted to 165 mM potassium acetate, 5 mM magnesium acetate, 5 mM $\beta$-mercaptoethanol and 10% (w/v) glycerol. *Staphylococcus aureus* V8 protease was then added at 1 $\mu$g for 30 $\mu$g topo II and the samples were incubated at 30°C for up to 60 min. After extraction with phenol and ether (see following section), the samples were dried and solubilized in 50 $\mu$l of 70 mM Tris-HCl (pH 7.6), 10 mM $MgCl_2$, 5 mM DTT containing 25 $\mu$Ci [$\gamma$-$^{32}$P]ATP and T4 polynucleotide kinase (8 U) and incubated at 37°C for 45 min. The samples were extracted again with phenol and ether, dried and prepared for SDS-PAGE.

*2.4. Phenol–ether extraction of crosslinked complexes*

Sequential extraction with phenol and ether was used to separate

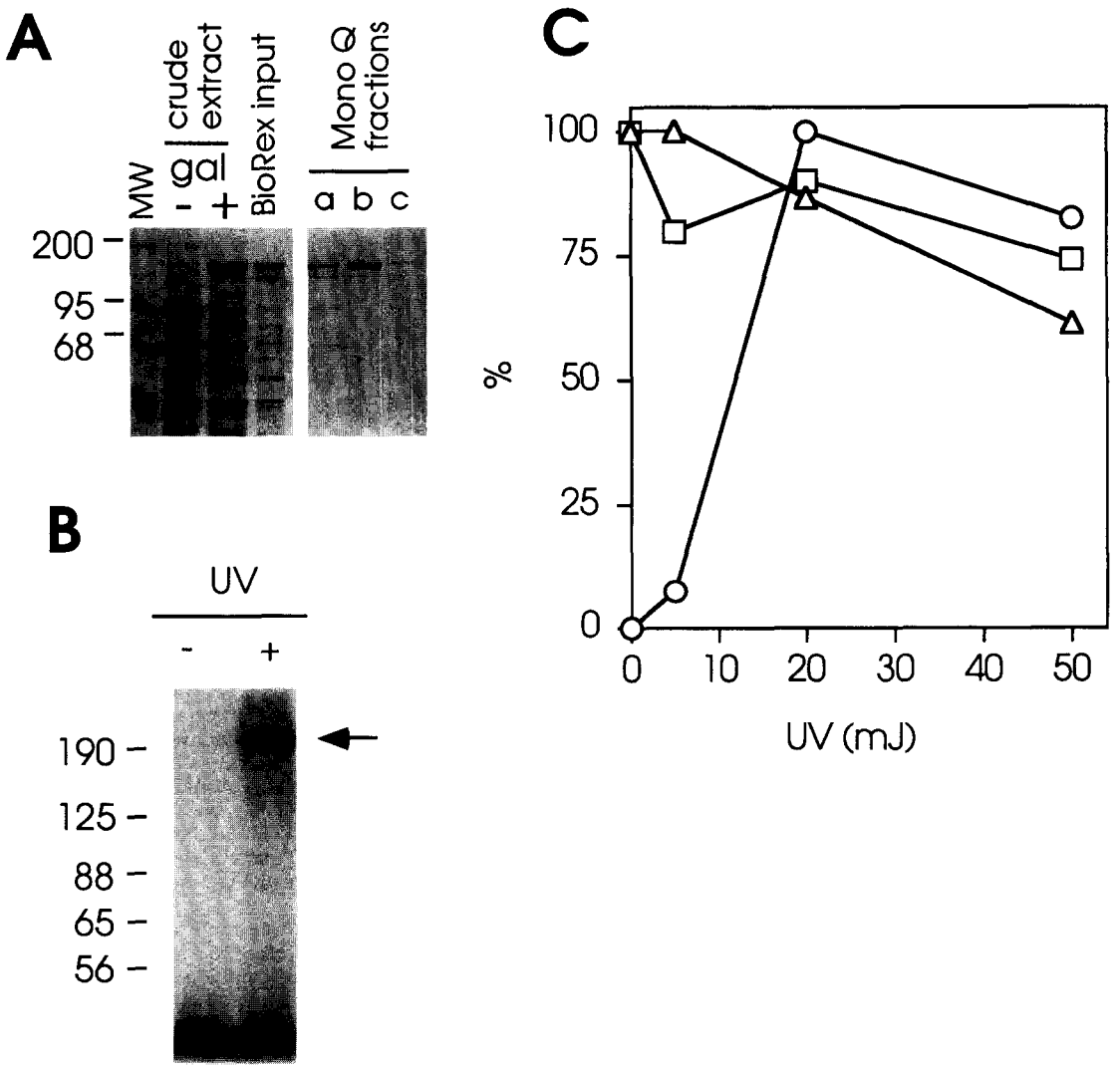


Fig. 1. Topo II purification and effect of UV irradiation on the formation of crosslinked topo II–DNA complexes and on topo II and DNA integrity. (A) Yeast cells carrying plasmid pYept2 were treated or not with galactose to induce topo II expression and crude extracts were prepared (see section 2). Topo II was purified by chromatography on BioRex (BioRex input) and Mono-Q columns. Mono-Q fractions a, b and c correspond to the left shoulder, the peak, and the right shoulder of the peak of topo II activity. Fraction b, which contains a single band at about 160 kDa, was used for all crosslinking experiments. The fractions were analysed by SDS-PAGE followed by staining with Coomassie blue. (B) Standard binding reactions (see section 2) were incubated for 3 min before irradiation with 0 (−UV) or 20 mJ (+UV). The crosslinked complexes were separated by SDS-PAGE and visualized by autoradiography. The arrow shows the crosslinked complex at about 200 kDa. The migration of protein standards, in kDa, is shown to the left. (C) Effect of UV irradiation on the formation of crosslinked complexes (circles), the integrity of topo II (squares), and the integrity of RY oligo (triangles). The radioactivity associated with the crosslinked complexes is expressed as percent of the maximal value obtained. The amount of intact topo II and RY oligo is expressed as percent of the value of unirradiated samples.

crosslinked topo II–DNA complexes from nucleotides. Samples were adjusted to 100 μl with water, an equal volume of phenol was added and the samples were vortexed vigorously for 20 s. After 5 min centrifugation at 12,000 × g, the upper aqueous phase was discarded and the phenol phase was extracted up to 4 additional times with water. Two volumes of ether were added to the washed phenol phase, and the samples were vortexed and centrifuged as above. The upper organic phase was discarded and the lower, aqueous phase was extracted twice with ether to remove residual phenol. The washed aqueous phase was dried by centrifugation under reduced pressure [18].

*2.5. Gel electrophoresis and analysis of crosslinked complexes*

Immediately after irradiation, samples were mixed with 1/3 vol of 4 × SDS loading buffer (200 mM Tris-HCl (pH 6.8), 8% SDS, 0.4% bromophenol blue, 40% glycerol, 1% β-mercaptoethanol, 4 M urea) and boiled for 2 min. The samples were analysed by SDS-PAGE in 8% gels with 4% stacking gels [17]. After 30 min electrophoresis at 200 V, the gels were dried onto blotting paper and exposed to Kodak X-AR film. Quantitation was obtained by laser scanning densitometry of bands obtained from autoradiograms exposed without intensifying screens, using a Molecular Dynamics Series 300 densitometer, or with a Molecular Dynamics PhosphorImager. In some experiments, proteins were silver stained as in [19].

## 3. Results and discussion

Highly purified *S. cerevisiae* topo II (Fig. 1A) was incubated in the absence of ATP with [$^{32}$P]RY oligo, consisting of 32 bp of alternating purines and pyrimidines, which is efficiently cleaved by topo II. An aliquot of the binding reaction was left unirradiated or was irradiated with a single 5 ns pulse of 266 nm light at 20 mJ. SDS loading buffer was added immediately and the samples were analysed by SDS-PAGE and autoradiography. Fig. 1B shows that UV irradiation caused the appearance of a radiolabelled band at about 200 kDa. This corresponds roughly to the sum of the masses of a topo II monomer (160 kDa) and the 32 bp RY oligo (20.7 kDa), as reported previously for other crosslinked protein–DNA complexes [16]. We also irradiated binding reactions with a single pulse of differing intensity, separated the crosslinked complexes by SDS-PAGE, and quantitated them by laser scanning densitometry of the autoradiographs (Fig. 1C). The appearance of the crosslinked complexes was dependent on irradiation and was maximal with a 20 mJ pulse. It was also dependent on the presence of topo II and of the DNA probe (see later sections).

We next examined the effect of UV irradiation on the integrity of topo II and RY oligo. Topo II was irradiated as above, the protein was separated by SDS-PAGE, and the amount of full-length protein was determined by densitometry after silver-staining of the protein. Irradiation doses between 10 and 50 mJ resulted in less than 25% topo II degradation (Fig. 1C). Similarly, radioactively labelled RY oligo was irradiated, electrophoresed through a non-denaturing polyacrylamide gel and the amount of full-length RY oligo was determined by quantitation of autoradiographs. Irradiation doses above 10 mJ caused a steady increase in RY oligo degradation (Fig. 1C). Most of the subsequent studies described here were performed with one pulse of 20 mJ, which gave about 0.25% crosslinking efficiency, while causing less than 15% degradation of topo II and RY oligo.

It has been shown that crosslinking induced by nanosecond or picosecond UV lasers takes place within 1 μs, well below the 100 μs time scale of microconformational transitions of macromolecules [20–22]. Therefore, the experimental conditions described above are well-suited for the study of binding kinetics and of the effect of DNA topology, which is sensitive to UV, on topo II binding. [$^{32}$P]RY oligo (6.25 nM) was incubated with excess topo II (8.5 nM) for different times before UV irradiation. Crosslinked complex formation was essentially complete by 7 s incubation. An association rate constant ($k_a$) of $3.2 \pm 1.1 \times 10^7$ $M^{-1} \cdot s^{-1}$was determined from 2 experiments as described in Cleat and Hay [23]. Dissociation of topo II–DNA complexes was measured by first incubating $^{32}$P-labelled RY oligo with excess topo II as above. After 30 s incubation, a 16-fold excess (100 nM) of unlabelled RY oligo was added and the samples were irradiated at different times. Dissociation was half-maximal at about 7 s. Data from two such experiments were used to determine a dissociation rate constant ($k_{diss}$) of

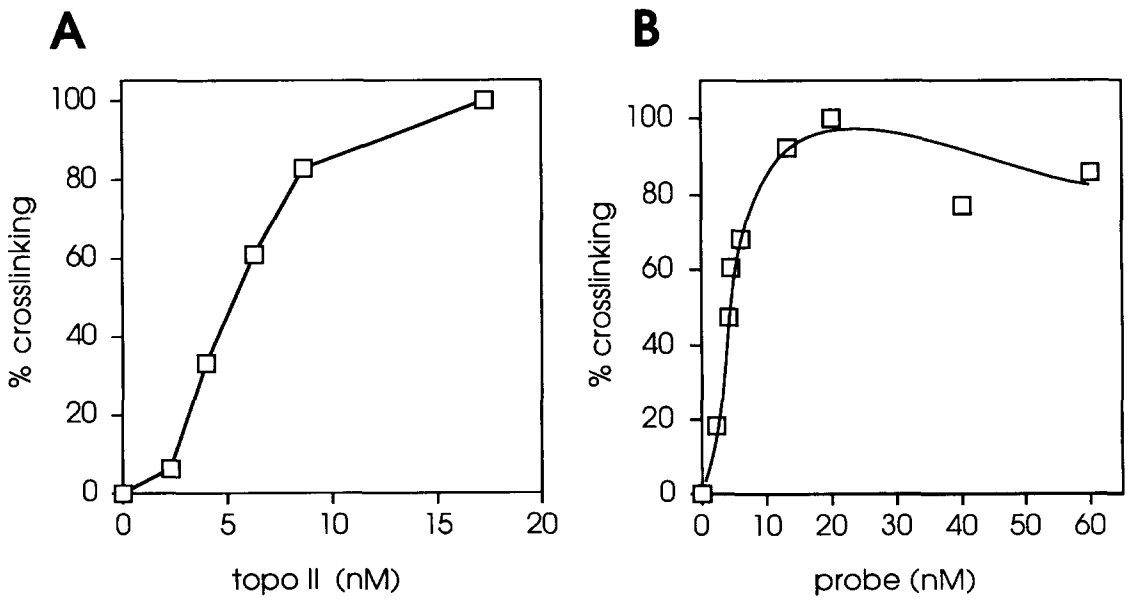


Fig. 2. Effect of topo II and DNA concentration on the formation of crosslinked complexes. Standard binding reactions containing a fixed concentration of RY oligo (25 nM) and different concentrations of topo II (A) or containing a fixed concentration of topo II (11 nM) and different concentrations of RY oligo (B), were assembled and irradiated, and the crosslinked complexes were analysed as in Fig. 1.

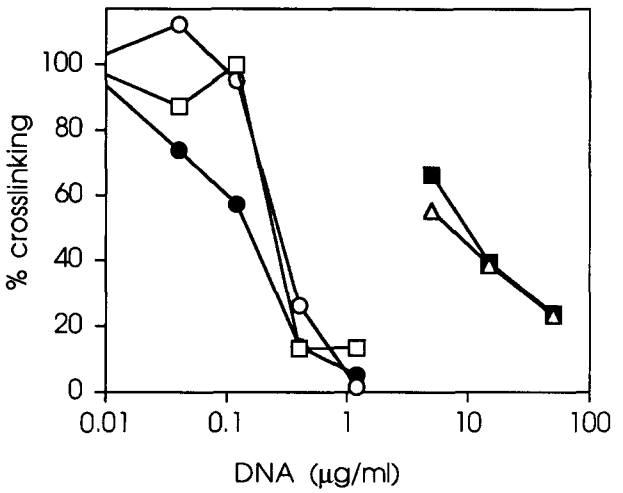


Fig. 3. Effect of DNA length and topology on the formation of crosslinked complexes. Standard binding reactions containing [$^{32}$P]RY oligo and different concentrations of unlabelled RY oligo (filled squares), non-RY oligo (triangles), supercoiled pRYG (filled circles), relaxed pRYG (open circles), or linear pRYG (open squares) were assembled, irradiated and the crosslinked complexes were analysed as in Fig. 1.

$0.26 \pm 0.04\ s^{-1}$. This permitted the determination of the equilibrium binding constant ($K_{eq}=k_a/k_{diss}$) at $1.2 \pm 0.5 \times 10^8\ M^{-1}$.

The dependence of crosslinking efficiency on the composition of the binding buffer was also measured. Maximal binding was observed in 50 mM Tris-HCl (pH 8.0), 50 mM NaCl and 1 mM EDTA, where the NaCl is contributed solely by the topo II storage buffer. Raising NaCl to 100 mM reduced significantly the formation of crosslinked complexes (not shown). All binding reactions were performed in the absence of divalent cations to prevent DNA cleavage by topo II [24,25].

We then determined the effect of topo II concentration and of RY oligo concentration on the formation of crosslinked complexes. Binding reactions containing a constant concentration of RY oligo and increasing topo II concentration were irradiated after 3 min incubation (Fig. 2A). No crosslinked complexes were observed in the absence of topo II. The formation of crosslinked complexes increased with increasing topo II concentration and was half-maximal at 6 nM. Similarly, binding reactions containing a constant concentration of topo II and increasing concentration of RY oligo were irradiated. No crosslinked complexes were detected in the absence of RY oligo. The formation of labelled crosslinked complexes was half-maximal at 5 nM and maximal at 20 nM (Fig. 2B).

We next used the formation of crosslinked topo II–[$^{32}$P]RY oligo complexes in competition assays to determine the affinity of topo II for DNA of differing sequence, size, and topological state. Topo II (11 nM) was incubated simultaneously with 25 nM [$^{32}$P]RY oligo and with increasing concentrations of unlabelled RY oligo or non-RY oligo, which contains a sequence not cleaved efficiently by topo II. Both oligodeoxyribonucleotide duplexes competed similarly, with half-maximal competition obtained at about 10 μg/ml, or about 12 nM (Fig. 3). This indicates that topo II does not bind with higher affinity to sequences that are cleaved strongly over sequences that are cleaved weakly.

Plasmid pRYG, from which the 32 bp RY oligo and non-RY oligo were derived, was also used in competition assays. The plasmid, in its negatively supercoiled form, relaxed by topo I, or linearized by restriction enzyme digestion, competed much more efficiently with the formation of topo II–$^{32}$P-labelled RY oligo complexes than either RY oligo or non-RY oligo (Fig. 3). Half-maximal competition was obtained at 0.15 μg/ml for supercoiled plasmid, and 0.3 μg/ml for both relaxed and linear plasmid, or about 0.2 nM and 0.1 nM plasmid, respectively. Spitzner et al. [14] have shown that pRYG does not contain strong topo II cleavage sites other than those in the RY insert. Thus, it is unlikely that the apparent increased binding affinity of the plasmid is due to the presence of additional cleavage sites within the plasmid. Taken together, our results indicate that topo II binds short DNA duplexes with rather high affinity ($K_{eq}=1 \times 10^8\ M^{-1}$) irrespective of whether they contain strong cleavage sites. Topo II binds much more efficiently to long DNA molecules with highest affinity for supercoiled DNA. This indicates that DNA topology is a more important determinant of topo II binding than DNA sequence. Yeast topo II has been shown to bind supercoiled DNA more strongly than relaxed DNA by a factor of two to three [26]. *Drosophila* and mammalian topo II also bind supercoiled DNA preferentially [7,27]. Roca et al. [8] have shown that binding of yeast topo II to DNA crossings is significant, especially in low salt, which is the condition we used. This suggests that increased affinity and crosslinking efficiency are due to increased density of crossings in supercoiled DNA.

Finally, we used this crosslinking technique to identify topo II region(s) which interact with DNA. The standard crosslinking protocol described above results in the formation of complexes with an electrophoretic mobility corresponding roughly to the sum of the molecular mass of the protein and DNA components (Fig. 1B). It was modified as follows to minimize the effect of the crosslinked DNA on the mobility of the complexes in SDS gels: topo II was incubated with unlabelled RY oligo and irradiated to form crosslinked complexes. DNA was then digested extensively with micrococcal nuclease, and the complexes were subjected to limited digestion with V8 protease as previously described [28]. The proteolysed crosslinked complexes were then purified, their short crosslinked DNA tag was labelled with $^{32}$P using polynucleotide kinase, and the complexes were analysed by SDS-PAGE and autoradiography (see section 2).

Limited digestion of crosslinked topo II-DNA complexes with V8 protease gave rise to a well-defined band at 29 kDa and a smear below 20 kDa (Fig. 4A). These were not observed when samples were not irradiated (Fig. 4A), when topo II or DNA were omitted from the binding reaction, or when samples were not digested with V8 (not shown). The labelled 29-kDa band was transferred quantitatively to nitrocellulose by electroblotting, suggesting that it did not consist of incompletely digested RY oligo. In addition, it could not have been caused by crosslinking of ATP to topo II because polynucleotide kinase cannot label mononucleotides and because the labelled band required the presence of intact DNA (not shown). The 29-kDa crosslinked complex comigrated with a topo II fragment whose amino-terminal sequence was determined as X-Ile-Leu-Phe, where X indicates an uncertainty in the identification of the amino acid residue. This corresponds to cleavage by V8 protease at Glu-680, which is followed by Leu-Ile-Leu-Phe, in agreement with the results of Lindsley and Wang [28] which

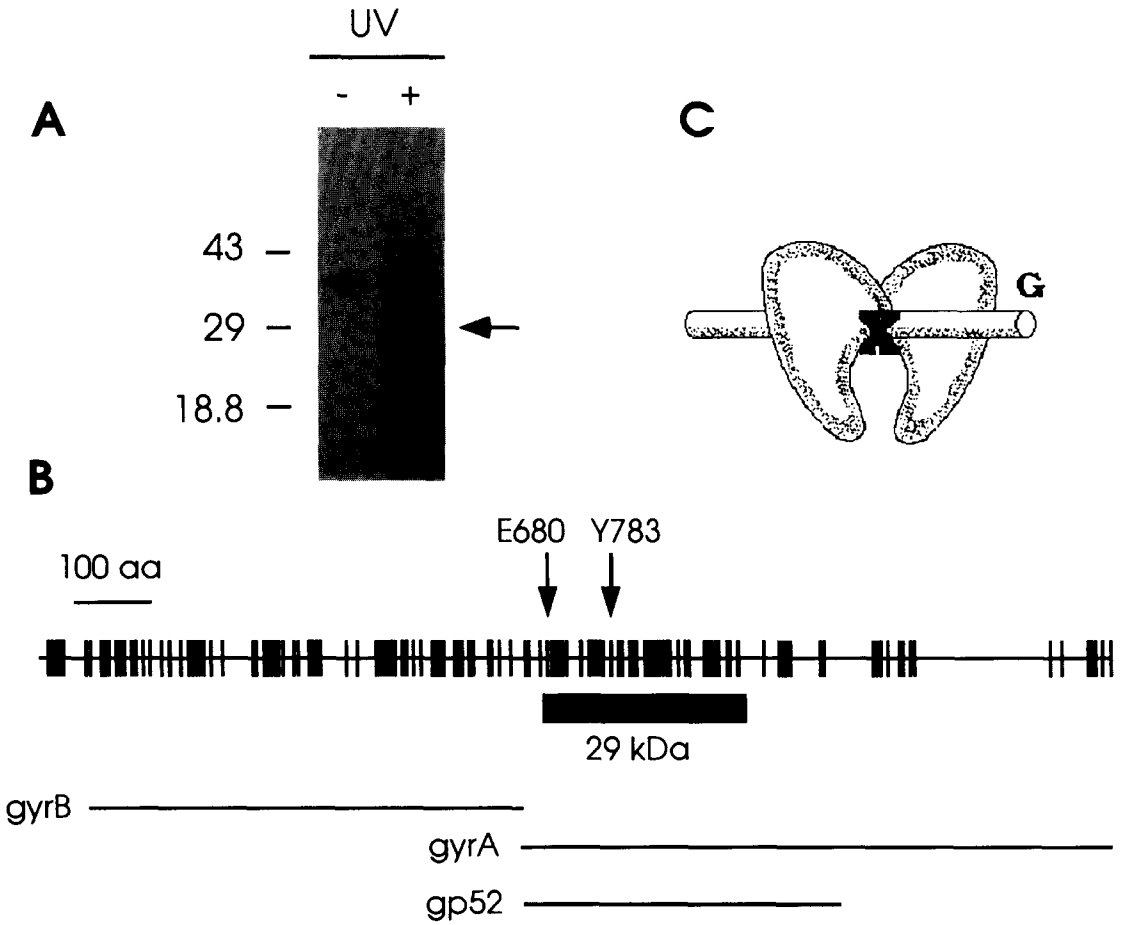


Fig. 4. A conserved 29-kDa DNA-binding domain in *S. cerevisiae* topo II. (A) Topo II was incubated with DNA and irradiated (+UV) or not (−UV). The reactions were digested with V8 protease for 60 min and the crosslinked proteolytic fragments were labelled and detected as described in section 2. The arrow points to the crosslinked 29-kDa fragment. The migration of protein standards, in kDa, is shown to the left. The radiolabelled band at about 38 kDa was considered nonspecific because it was observed in the absence of UV irradiation (first lane) or V8 protease digestion (not shown). (B) Diagram of the amino acid sequence of *S. cerevisiae* topo II and regions of similarity to GyrB, GyrA and gp52. Vertical bars represent positions in *S. cerevisiae* topo II which are at least 70% homologous in over 30 type II DNA topoisomerases, as determined from Fig. 3 of [11]. The 29-kDa region marked by the black box represents the region crosslinked to DNA described in this study. E680 is the site cut by V8 protease and Y783 is the active site Tyr. (C) Model depicting the interaction of the G DNA segment with topo II and a possible crosslinking site in the open clamp conformation of Roca and Wang [26]. In the absence of ATP, the clamp is open and topo II can bind the G segment (G). The X shows crosslinking at a site of contact between the G segment in the 29-kDa region postulated to form part of the inside of the clamp.

also show a prominent V8 protease site at Glu-680. However, these authors obtained a 60-kDa proteolytic fragment [28] whereas we obtain a 29-kDa fragment. The reason for this discrepancy is not known but since the 60-kDa fragment and the 29-kDa fragment are both partial digestion products, it is likely that the 29-kDa fragment resulted from more extensive digestion. The smear below 20 kDa could represent additional digestion products of the crosslinked 29-kDa fragment or distinct sites of protein–DNA crosslinking, but this was not studied further here.

Interestingly, Glu-680 is in the junction of the GyrB- and GyrA-like domains (Fig. 4B). The 29-kDa fragment contains the active Tyr-783 and is homologous to the N-terminal region of bacterial GyrA and T4 gp52. The N-terminus of the 29-kDa topo II fragment aligns well with that of GyrA and gp52, suggesting that it represents a structurally and functionally related domain in topo II (Fig. 4B). The 29-kDa topo II fragment identified in this study is homologous to amino acids 22–309 of GyrA. Limited digestion of GyrA by trypsin releases an N-terminal fragment of 64 kDa that supports DNA supercoiling [29], and deletion studies show that the smallest GyrA fragment capable of enzyme activity contains amino acids 7–523, implying the existence of a DNA-binding domain in this region of GyrA.

According to the ATP-dependent protein clamp model of Roca and Wang [26], in the absence of ATP, the topo II dimer forms an open clamp which can bind the G DNA segment, whose strands will be cleaved, and the T segment, which will be transported through the cleaved G segment. Since our binding experiments were performed without ATP or divalent cations, crosslinking presumably occured at a site of interaction between an uncleaved DNA segment, possibly the G segment, and the open topo II clamp. If this is the case, our results would predict that the 29-kDa topo II region that becomes crosslinked

to DNA contains amino acid residues that project to the inside of the protein clamp and serve to bind DNA as depicted in the model shown in Fig. 4C.

*Acknowledgements:* We thank Hilary Anderson, Patrick Gowdy, Duncan Ho and Geoffrey Stone for discussions and critical reading of the manuscript and Jamie Piret for use of the scanning densitometer. This work was supported by a grant from the Medical Research Council of Canada to M.R., who is a Scholar of the Medical Research Council of Canada. M.T.M. received support from the NIH Senior Fogarty International Fellowship and from NIH Grant AI28362.

## References

[1] Wang, J.C. (1991) J. Biol. Chem. 266, 6659–6662.
[2] DiNardo, S., Voelkel, K. and Sternglanz, R. (1984) Proc. Natl. Acad. Sci. USA 81, 2616–2620.
[3] Uemura, T., Ohkura, H., Adachi, Y., Morino, K., Shiozaki, K. and Yanagida, M. (1987) Cell 50, 917–925.
[4] Holm, C., Stearns, T. and Botstein, D. (1989) Mol. Cell. Biol. 9, 159–168.
[5] Rose, D., Thomas, W. and Holm, C. (1990) Cell 60, 1009–1017.
[6] Anderson, H.J. and Roberge, M. (1992) Cell Biol. Int. Reports 16, 717–724.
[7] Zechiedrich, E.L. and Osheroff, N. (1990) EMBO J. 9, 4555–4562.
[8] Roca, J., Berger, J.M. and Wang, J.C. (1993) J. Biol. Chem. 268, 15250–14255.
[9] Osheroff, N., Corbett, A.H. and Robinson, M.L. (1994) Adv. Pharmacol. 29B, 105–126.
[10] Shiozaki, K. and Yanagida, M. (1991) Mol. Cell. Biol. 11, 6093–6102.
[11] Caron, P.R. and Wang, J.C. (1994) Adv. Pharmacol. 29B, 271–297.
[12] Caron, P.R. and Wang, J.C. (1993) in: Molecular Biology of DNA Topoisomerases and its Applications to Chemotherapy (Andoh, T., Ikeda, H. and Oguro, M. eds.) pp. 1–18, CRC Press, Boca Raton.
[13] Lynn, R., Giaver, G., Swanberg, S.L. and Wang, J.C. (1986) Science 233, 647–649.
[14] Spitzner, J.R., Chung, I.K. and Muller, M.T. (1990) Nucleic Acids Res. 18, 1–11.
[15] Adachi, Y., Käs, E. and Laemmli, U.K. (1989) EMBO J. 8, 3997–4006.
[16] Ho, D.T., Sauvé, D.M. and Roberge, M. (1994) Anal. Biochem. 218, 248–254.
[17] Sambrook, J., Fritsch, E.F. and Maniatis, T. (1989) Molecular Cloning: a Laboratory Manual, 2nd edn., Cold Spring Harbor University Press, Cold Spring Harbor, NY.
[18] Sauvé, D.M., Ho, D.T. and Roberge, M. (1995) Anal. Biochem. 226, 382–383.
[19] Bonifacino, J.S. (1989) in: Current Protocols in Molecular Biology (Ausubel, F.H., Brent, R., Kingston, R.E., Moore, D.D., Seidman, J.G., Smith, J.A. and Struhl, K. eds.) pp. 10.18.1–10.18.9, Wiley, New York.
[20] Careri, G., Fasella, P. and Gratton, E. (1975) CRC Crit. Rev. Biochem. 3, 141–164.
[21] Hockensmith, J.W., Vorachek, W.R., Evertsz, E.M. and von Hippel, P.H. (1991) Methods Enzymol. 208, 211–236.
[22] Pashev, I.G., Dimitrov, S.I. and Angelov, D. (1991) Trends Biol. Sci. 16, 323–326.
[23] Cleat, P.H. and Hay, R.T. (1989) FEBS Lett. 258, 51–54.
[24] Sander, M. and Hsieh, T.-S. (1983) J. Biol. Chem. 258, 8421–8428.
[25] Osheroff, N. (1987) Biochemistry 26, 6402–6406.
[26] Roca, J. and Wang, J.C. (1992) Cell 71, 833–840.
[27] Pommier, Y., Kerrigan, D. and Kohn, K. (1989) Biochemistry 28, 995–1002.
[28] Lindsley, J.E. and Wang, J.C. (1991) Proc. Natl. Acad. Sci. USA 88, 10485–10489.
[29] Reece, R.J. and Maxwell, A. (1991) J. Biol. Chem. 266, 3540–3546.